Table 1. Signal intensity of β-actin and GAPDH.

Value type	Gene Title	Papilla			Medulla			Cortex			Whole		
		No.1	No.2	No.3	No.1	No.2	No.3	No.1	No.2	No.3	No.1	No.2	No.3
Signal intensity	β-actin	19619	20290	18700	20158	22911	20379	19881	23365	20759	19277	19278	21390
	GAPDH	17008	16029	15284	20169	21086	20291	22338	23834	23006	20765	20430	20458
Signal intensity	β-actin	0.95	0.98	0.90	0.98	1.11	0.99	0.96	1.13	1.00	0.93	0.93	1.03
Mean of signal intensity	GAPDH	0.85	0.81	0.77	1.01	1.06	1.02	1.12	1.20	1.16	1.04	1.03	1.03

Expression of β-actin and GAPDH in the three portions of kidney slice, papilla, medulla, and cortex, from three different rats (No. 1 - 3) as well as in the whole slice of three different rats (No. 4 - 6). Signal intensity of each gene was divided by the mean of all probes in the chip multiplied by 500 (global mean normalization, upper columns), after which each value was divided by the mean of these 12 values (per gene normalization).

in all samples of papilla but absent in all of medulla and cortex were 448, and only 27 (6%) were all present in the whole slice. Genes with present call in all samples of medulla but absent in others were quite rare, i.e., 18 probe sets, of which 2 (11%) had present call in all of the whole slices. Cortex-specific probes were found to be 44, and 34 (77%) were present in all of the samples of the whole slice. The relatively small number in the latter two portions indicates that most of the genes are common between medulla and cortex, and the gene expression in papilla is unique. These results suggest again that the region specific genes (in other than cortex) are difficult to detect by analysis of the whole slice.

The above results clearly indicate that the population of genes expressed in each region is quite different. Theoretically, absolute values of expression should be used when an accurate comparison is made between regions with different total mRNA contents. In order to further elucidate this point, the "percellome procedure" was employed to compare with global normalization.

The mean of copy numbers (or the values directly related to copy numbers) of β-actin was calculated to be 234, 291, 341, and 309 in papilla, medulla, cortex and the whole slice, respectively, i.e., the ratio in papilla, medulla, and cortex (whole slice = 1) was 0.76, 0.94 and 1.10, respectively. The mean of copy numbers of GAPDH was calculated to be 208, 298, 369 and 343, in papilla, medulla, cortex and the whole slice, respectively, i.e., the ratio in papilla, medulla, cortex (whole slice = 1) was 0.61, 0.87 and 1.08, respectively. These

Table 2. Pearson's correlation coefficient between samples.

A		Papilla			Medulla			Cortex			Whole		
		No1	No2	No3	No1	No2	No3	No1	No2	No3	No4	No5	No6
Papilla	No1	1	0.989	0.986	0.847	0.843	0.837	0.765	0.758	0.761	0.814	0.811	0.812
	No2		1	0.985	0.853	0.853	0.846	0.778	0.773	0.775	0.827	0.825	0.825
	No3			1	0.815	0.812	0.811	0.738	0.73	0.735	0.789	0.785	0.786
Medulla	No1				1	0.994	0.991	0.947	0.933	0.937	0.958	0.967	0.956
	No2					1	0.991	0.943	0.935	0.938	0.957	0.968	0.955
	No3						1	0.953	0.943	0.953	0.964	0.972	0.962
Cortex	No1							1	0.991	0.992	0.986	0.983	0.986
	No2								1	0.991	0.983	0.979	0.984
	No3									1	0.984	0.98	0.985
Whole	No4										1	0.996	0.994
	No5											1	0.992
	No6												1

0.90 –
0.85 –
0.80 –
0.75 –
– 0.75

B		Papilla			Medulla			Cortex			Whole		
		No1	No2	No3	No1	No2	No3	No1	No2	No3	No4	No5	No6
Papilla	No1	1	0.989	0.985	0.837	0.833	0.826	0.755	0.755	0.752	0.801	0.797	0.801
	No2		1	0.982	0.843	0.844	0.834	0.768	0.769	0.764	0.813	0.81	0.814
	No3			1	0.801	0.798	0.795	0.725	0.723	0.724	0.771	0.766	0.77
Medulla	No1				1	0.994	0.991	0.946	0.934	0.937	0.957	0.967	0.955
	No2					1	0.991	0.942	0.936	0.937	0.956	0.967	0.954
	No3						1	0.953	0.945	0.953	0.963	0.971	0.961
Cortex	No1							1	0.992	0.992	0.987	0.984	0.986
	No2								1	0.992	0.986	0.982	0.986
	No3									1	0.985	0.981	0.985
Whole	No4										1	0.996	0.994
	No5											1	0.992
	No6												1

0.90 –
0.85 –
0.80 –
0.75 –
– 0.75

A: Calculated on the data of global normalization.
B: Calculated on the data of percellome.

values clearly differ from those by global normalization, namely, the expression values in papilla were apparently overestimated by global normalization. The correlation coefficients calculated from the values normalized by percellome (Table 2B) were almost identical to that in Table 2A except between papilla and others, which showed a relatively large decrease in value. These results again indicated that global normalization was problematic, especially for papilla among the portions, most possibly because of the low amount of mRNA production in that region, compared with others.

After normalization either by global mean or percellome, the genes with absent call in all the samples were discarded and analyzed by ANOVA ($p<0.01$) in order to extract probe sets showing different expression in any region(s). The numbers of extracted probe sets were 12,322 for percellome and 8,161 for global normalization. Fig. 3 shows the results of K-means clustering (Euclidean, 10 clusters) of the expression values converted into z-scores in order to see the trend of expression in each region.

By percellome normalization (Fig. 3A), clusters of probe sets with characteristic region-dependent expression were efficiently extracted. It was also obvious from the figure that there was only one cluster containing only 293 probe sets that showed specifically high expression in papilla, and the other probe sets showed the lowest value in papilla compared to any other clusters. This indicates that most of the probe sets showed the lowest expression in papilla and the highest ones were exceptional. On the other hand, the clusters of global normalization (Fig. 3B) showed various, inconsistent patterns. Contrasting with the case of percellome normalization, there were many clusters in which gene expression was highest in papilla, or where papilla was equivalent to other region(s).

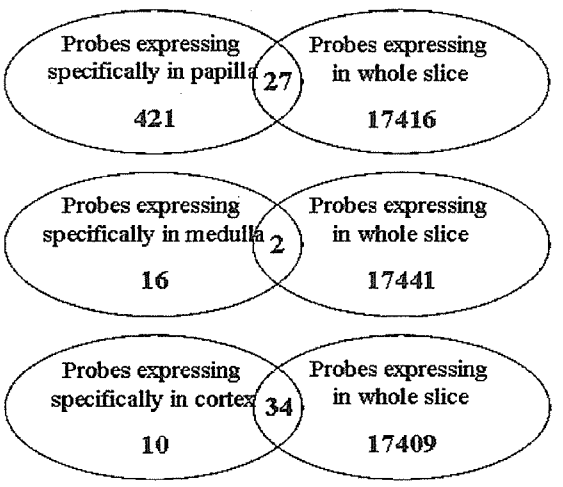

Fig. 2. Venn diagram of region-specific genes extracted by flags (present, absent and marginal call). The probes having "present call" in all samples of papilla and "absent call" in all samples of medulla and cortex were considered to be papilla-specific. The medulla- and cortex-specific probes were also extracted in the same manner and examined whether they were absent in the whole slice.

An obvious contradiction was noted between the two normalizations as described above, so further comparison was made. After the elimination of the probe sets that had absent call in all samples, the probe sets were classified into categories where the values showed maximum or minimum. Fig. 4 shows their counts in papilla, medulla, cortex, and whole slice for each normalization method. In the case of percellome normalization (A), the numbers of probe sets showing a maximal value were dominantly found in cortex, while the most of those showing a minimum were in papilla. On the other hand, in the case of global normalization (B), many of the probe sets showing their maximum were in papilla, while the numbers of probe sets with minimal expression were distributed evenly among the samples. It is noteworthy that very many (>3,000) probe sets showed minimal expression in the whole slice. However, this is theoretically impossible because the whole slice contains all the other 3 portions. Therefore, it should be concluded that the extraction of the genes with region-specific expression based on global normalization gives an error, and thus percellome normalization should be used in this case.

Based on the above results, region-specific genes in kidney were extracted as follows. After selection by ANOVA ($p<0.01$) for the data of percellome normalization, genes were categorized by the position at which they showed the larger expression value and then aligned in the order of their ratio to the minimum, for papilla (Table 3), medulla (Table 4) and cortex (Table 5). As is obvious from Figs. 3 and 4, the production of mRNA per cell was considered to be in the order of cortex>medulla>papilla, and the numbers of region-specific probe sets were also in this order. For simplicity, probe sets without any annotation were eliminated, and the ones with the ratio of >3 for papilla, >10 for medulla, and >30 for cortex, are presented in the tables.

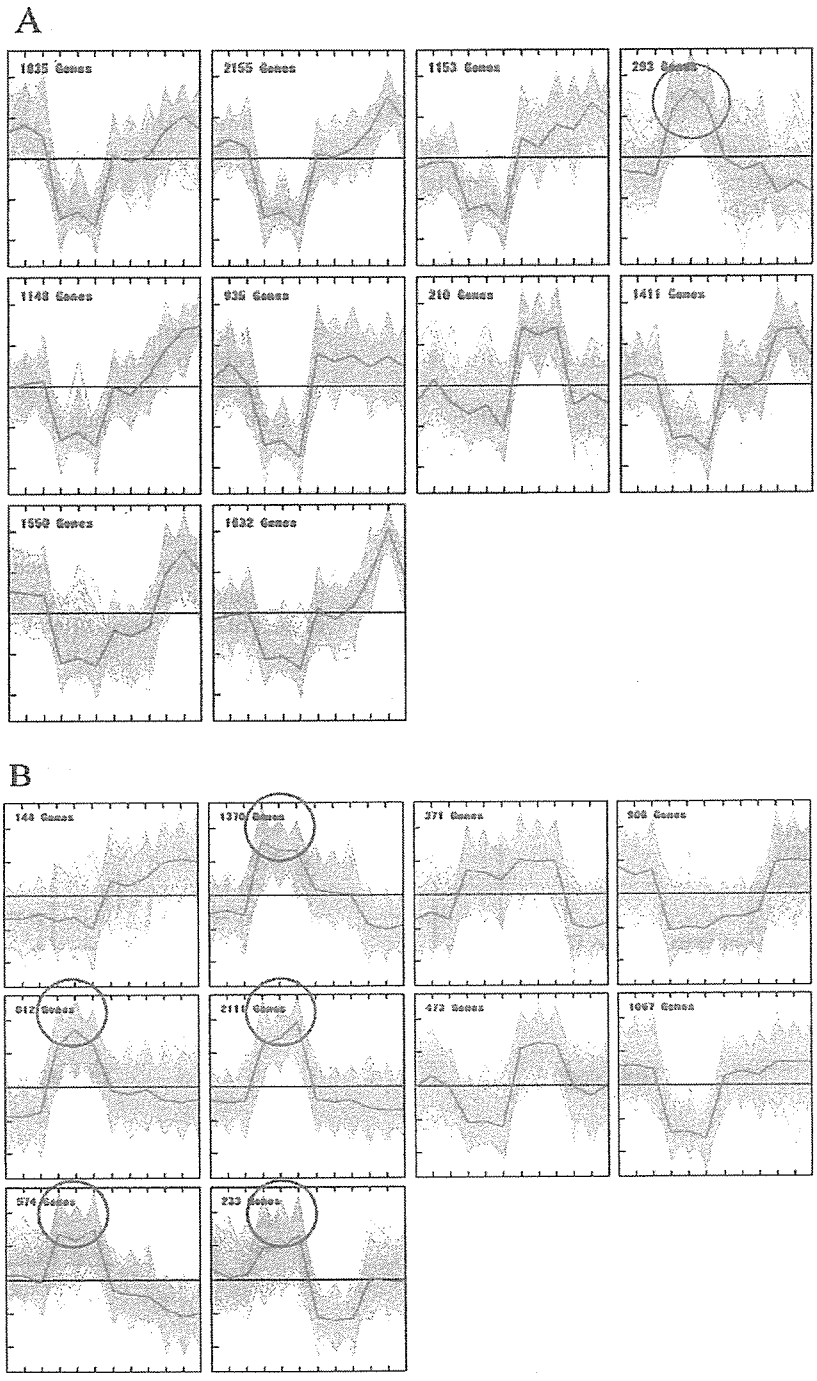

Fig. 3. K-means clustering of genes expressed in papilla, medulla, cortex, and whole slice of kidney. Data were processed by percellome normalization (A) or global mean normalization (B), and then converted into z-scores. K-means clustering (Euclidean, 10 clusters) was performed with MeV version 3.1 (The Institute for Genomic Research, Rockville, MD, USA). In each cluster, individual samples are aligned from left to right: whole slice (3), papilla (3), medulla (3), and cortex (3). Red lines indicatethe mean of the probes within each cluster. Orange circles indicate where papilla showed specifically high expression values.

In all these three tables, the higher rank is generally occupied by the genes related to channels, transporters and metabolic enzymes, suggesting that the gene lists are meaningful for analysis of specific renal functions.

In most of the papilla-enriched genes (Table 3), the ratio of papilla/cortex is larger than that of papilla/medulla, since the composition of papilla is closer to medulla than to cortex. The exceptional genes (highest in papilla and lowest in medulla) are shaded in the table. The outstanding feature of this table is that heat shock proteins and cytoskeleton/extracellular matrix proteins are present, in addition to the channel/transporters and metabolic enzymes.

In most of the medulla-enriched genes (Table 4), the ratio of medulla/cortex is less than 2, suggesting that their expression is relatively similar between these two portions. The genes with ratio of >3 are shaded in the table, but they are only 3 sets, indicating that medulla-specific genes are rare. The higher rank of the list in Table 4 is also occupied by channel/transporters and metabolic enzymes, and cytoskeletal proteins are scarce. A unique feature of medulla is the existence of 4 probe sets for prolactin receptor. This might occur simply because the quality of these multiple probes for one prolactin receptor is uniformly high.

Table 5 shows genes that showed the highest value in the cortex. It is noteworthy that many genes show more than 3 fold (shaded in the table) for the cortex/medulla ratio, indicating that there are many cortex-specific genes. The higher rank of this table is also occupied by channel/transporters and metabolic enzymes, but the numbers of metabolic enzymes are more prominent than in medulla.

Table 6 summarizes the genes categorized as channel/transporters, metabolic enzymes, cytoskeletons, and others for each portion.

DISCUSSION

The kidney is composed of various types of cells, and each portion (papilla, medulla, and cortex) has specific functions with wide variety, and the adverse effects of drugs vary with each portion. For example,

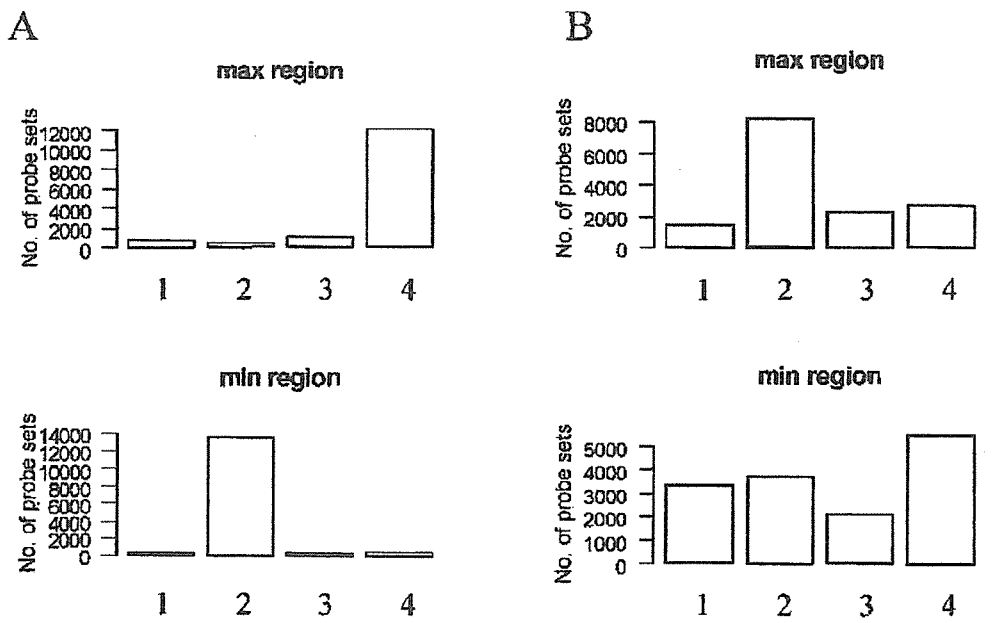

Fig. 4. The numbers of probe sets where their expression was maximal or minimal in whole slice, papilla, medulla, or cortex of kidney. After normalization by percellome (A) or global mean (B), probes with absent call in all samples were eliminated, and the numbers of probe sets with maximal (upper panels) or minimal (lower panels) were counted for each region, i.e., whole slice (1), papilla (2), medulla (3), and cortex (4).

Table 3. A list of probe sets specifically expressed in papilla of kidney.

Probe sets	papilla/ cortex	papilla/ medulla	medulla/ cortex	GENE_SYMBOL	GENE_NAME	channel transporter	Metabolic enzymes	cytoskeleton /extracellular matrix
1368259_at	32.0	12.7	2.5	Ptgs1	prostaglandin-endoperoxide synthase 1			
1389067_at	29.5	10.7	2.8	Slco4a1	solute carrier organic anion transporter family, member 4a1			
1372190_at	23.8	8.1	2.9	Aqp4	Aquaporin 4			
1394200_at	22.9	4.9	4.7	Hspa2	heat shock protein 2			
1387092_at	17.5	5.4	3.2	Fxyd4	FXYD domain-containing ion transport regulator 4			
1367847_at	17.4	5.4	3.2	Nupr1	nuclear protein 1			
1388460_at	16.8	5.6	3.0	Capg_predicted	capping protein (actin filament), gelsolin-like (predicted)			
1383469_at	7.2	14.6	0.5	Aldh1a3	Aldehyde dehydrogenase family 1, subfamily A3			
1376711_at	13.3	7.1	1.9	Cldn11	claudin 11			
1383319_at	13.2	2.5	5.3	Slc4a11_predicted	solute carrier family 4, sodium bicarbonate transporter-like, member 11 (predicted)			
1367734_at	13.1	7.9	1.7	Akr1b4	aldo-keto reductase family 1, member B4 (aldose reductase)			
1368765_at	10.7	2.5	4.2	Clcnk1	chloride channel K1			
1370229_at	10.5	1.9	5.4	Ndr4	N-myc downstream regulated 4			
1369841_at	10.3	4.2	2.4	Hspa2	heat shock protein 2			
1382303_at	3.8	8.8	0.4	RGD:1303187	phosphatase and actin regulator 1			
1378690_at	7.6	3.9	2.0	Ly6a_predicted	lymphocyte antigen 6 complex, locus A (predicted)			
1367661_at	6.8	3.7	1.8	S100a6	S100 calcium binding protein A6 (calcyclin)			
1374207_at	6.6	2.5	2.6	Agpt2	angiopoietin 2			
1369113_at	6.1	3.9	1.6	Grem1	gremlin 1 homolog, cysteine knot superfamily (Xenopus laevis)			
1368858_at	5.9	2.1	2.8	Ugt8	UDP-glucuronosyltransferase 8			
1368247_at	5.4	3.7	1.5	Hspa1a /// Hspa1b	heat shock 70kD protein 1A /// heat shock 70kD protein 1B			
1370334_at	3.2	5.4	0.6	Plekhb1	evectin-1			
1367650_at	5.1	3.1	1.6	Lcn7	lipocalin 7			
1374861_at	5.1	2.1	2.4	Tle2_predicted	transducin-like enhancer of split 2, homolog of Drosophila E(spl) (predicted)			
1387100_at	4.1	5.1	0.8	Aqp3	aquaporin 3			
1369949_at	5.0	3.6	1.4	Lu	Lutheran blood group (Auberger b antigen included)			
1369263_at	5.0	2.4	2.0	Wnt5a	wingless-type MMTV integration site 5A			
1370312_at	4.9	1.5	3.4	Spon1	spondin 1			
1388459_at	4.7	2.9	1.6	Col18a1	collagen, type XVIII, alpha 1			
1388456_at	4.3	3.0	1.4	S100a1	S100 calcium binding protein A1			
1393209_at	3.6	4.3	0.8	bsnd	Bartter syndrome, infantile, with sensorineural deafness (Barttin)			
1373733_at	4.3	2.8	1.5	Bok	Bcl-2-related ovarian killer protein			
1388547_at	4.2	2.5	1.7	Cldn4_predicted	claudin 4 (predicted)			

Table 3. Continued.

Probe sets	papilla/ cortex	papilla/ medulla	medulla/ cortex	GENE_SYMBOL	GENE_NAME	channel transporter	Metabolic enzymes	cytoskeleton /extracellular matrix
1396152_s_at	4.1	2.4	1.7	Igfbp5	insulin-like growth factor binding protein 5			
1367812_at	4.0	3.3	1.2	Spnb3	beta-spectrin 3			
1367577_at	3.4	3.9	0.9	Hspb1	heat shock 27kDa protein 1			
1372755_at	3.9	2.5	1.6	Mal2	mal, T-cell differentiation protein 2			
1370834_at	3.8	1.8	2.2	Hs3st1	heparan sulfate (glucosamine) 3-O-sulfotransferase 1			
1388155_at	3.8	3.3	1.2	Krt1-18	keratin complex 1, acidic, gene 18			
1372299_at	3.7	2.3	1.6	Cdkn1c	cyclin-dependent kinase inhibitor 1C (P57)			
1387886_at	3.6	2.7	1.3	Prelp	proline arginine-rich end leucine-rich repeat protein			
1368527_at	1.7	3.6	0.5	Ptgs2	prostaglandin-endoperoxide synthase 2			
1388102_at	1.9	3.5	0.5	Ltb4dh	leukotriene B4 12-hydroxydehydrogenase			
1370048_at	3.4	2.8	1.2	Edg2	endothelial differentiation, lysophosphatidic acid G-protein-coupled receptor, 2			
1371004_at	3.4	1.7	2.0	Sort1	sortilin 1			
1397830_at	3.4	2.3	1.5	Igfbp5	Insulin-like growth factor binding protein 5			
1369953_a_at	3.3	1.5	2.2	Cd24	CD24 antigen			
1367912_at	3.2	2.3	1.4	Ltbp1	latent transforming growth factor beta binding protein 1			
1387566_at	3.2	1.6	2.0	Pla2g4a	phospholipase A2, group IVA (cytosolic, calcium-dependent)			
1370912_at	3.2	2.3	1.4	Hspa1b	heat shock 70kD protein 1B			
1398318_at	3.2	2.1	1.5	Muc1	mucin 1, transmembrane			
1371625_at	3.1	2.8	1.1	Pygb	brain glycogen phosphorylase			
1370026_at	3.1	1.1	2.8	Cryab	crystallin, alpha B			
1393048_at	3.1	1.1	2.8	Adra2a	Adrenergic receptor, alpha 2a			
1388143_at	3.1	2.4	1.3	Col18a1	collagen, type XVIII, alpha 1			
1393958_at	3.1	2.1	1.5	Arhgap4	Rho GTPase activating protein 4			
1369084_a_at	3.1	2.8	1.1	Bok	Bcl-2-related ovarian killer protein			
1371499_at	3.0	1.8	1.7	Cd9	CD9 antigen			
1391830_at	3.0	1.9	1.6	Cpne8_predicted	copine VIII (predicted)			
1368342_at	3.0	1.9	1.6	Ampd3	adenosine monophosphate deaminase 3			
1384192_at	3.0	2.1	1.4	Chst1_predicted	carbohydrate (keratan sulfate Gal-6) sulfotransferase 1 (predicted)			
1398431_at	1.2	3.0	0.4	Car8_predicted	carbonic anhydrase 8 (predicted)			
1375170_at	3.0	1.6	1.9	S100a11_predicted	S100 calcium binding protein A11 (calizzarin) (predicted)			
1367759_at	3.0	1.2	2.5	H1f0	H1 histone family, member 0			
1387040_at	3.0	1.6	1.8	Mal	myelin and lymphocyte protein			

After selection by ANOVA ($p<0.01$) for the data of percellome normalization, genes maximally expressed in papilla were selected. The genes were aligned in the order of the ratio to the lower expression value, either in medulla or in cortex. As the genes listed here are expressed higher in medulla than cortex, in general, exceptional cases (ratio<0.6) are shaded in the medulla/cortex column. The genes categorized to "channel/transporters", "metabolic enzymes", or "cytoskeleton/extracellular matrix" are also shaded. Proteases or enzymes involving signal transduction are not included in the category of "metabolic enzymes". For simplicity, genes with less than 3-fold specificity are omitted.

Table 4. A list of probe sets specifically expressed in medulla of kidney.

Probe sets	medulla/ papilla	cortex/ papilla	medulla/ cortex	GENE_SYMBOL	GENE_NAME	channel transporter	Metabolic enzymes	cytoskeleton /extracellular matrix
1370377_at	204.8	124.5	1.6	Cyp2d9 /// Cyp2d10	cytochrome P450, family 2, subfamily d, polypeptide 9 /// cytochrome P450, family 2, subfamily d, polypeptide 10			
1387567_at	184.9	119.7	1.5	Slc21a1 /// LOC497799	solute carrier family 21, member 1 /// hypothetical gene supported by NM_017111			
1369401_at	153.0	69.6	2.2	Slc21a13	solute carrier family 21, member 13			
1387328_at	149.6	100.5	1.5	Cyp2c	Cytochrome P450, subfamily IIC (mephenytoin 4-hydroxylase)			
1368288_at	147.9	90.7	1.6	Gc	group specific component			
1368498_a_at	147.3	102.7	1.4	RGD:621387	kidney specific organic anion transporter			
1386454_at	133.0	46.7	2.8	Slc23a3_predicted	solute carrier family 23 (nucleobase transporters), member 3 (predicted)			
1370789_a_at	132.6	91.8	1.4	Prlr	prolactin receptor			
1387987_at	120.1	43.9	2.7	Slc22a19	solute carrier family 22 (organic anion transporter), member 19			
1390569_at	117.4	74.7	1.6	RGD:1359493	similar to carnosinase 1			
1369450_at	114.9	92.3	1.2	UST5r	integral membrane transport protein UST5r			
1369493_at	89.1	62.1	1.4	Prlr	prolactin receptor			
1368575_at	88.9	70.0	1.3	Slc6a18	solute carrier family 6 (neurotransmitter transporter), member 18			
1370824_at	88.2	60.3	1.5	Slc38a3	solute carrier family 38, member 3			
1387382_at	88.0	42.0	2.1	Hnmt	histamine N-methyltransferase			
1387303_at	83.1	59.2	1.4	Slc22a2	solute carrier family 22 (organic cation transporter), member 2			
1378247_at	81.5	41.3	2.0	Eaf2	ELL associated factor 2			
1373990_at	78.5	24.0	3.3	Slc7a12_predicted /// LOC361914	solute carrier family 7 (cationic amino acid transporter, y+ system), member 12 (predicted) /// similar to solute carrier family 7 (cationic amino acid transporter, y+ system), member 12			
1389756_at	78.0	57.9	1.3	Melk_predicted	maternal embryonic leucine zipper kinase (predicted)			
1384775_s_at	74.6	51.7	1.4	Tmprss8	transmembrane protease, serine 8 (intestinal)			
1370384_a_at	73.9	60.3	1.2	Prlr	prolactin receptor			
1368208_at	72.9	60.3	1.2	Cml1	camello-like 1			
1376944_at	72.5	68.6	1.1	Prlr	Prolactin receptor			
1385132_at	69.0	32.5	2.1	Mybl1_predicted	myeloblastosis oncogene-like 1 (predicted)			
1368651_at	66.4	49.0	1.4	Pklr	pyruvate kinase, liver and RBC			
1368304_at	65.8	57.1	1.2	Fmo3	Flavin containing monooxygenase 3			
1397205_at	54.9	42.8	1.3	Dhrs7_predicted /// LOC500672	dehydrogenase/reductase (SDR family) member 7 (predicted) /// similar to Down-regulated in nephrectomized rat kidney #3			

Table 4. Continued.

Probe sets	medulla/ papilla	cortex/ papilla	medulla/ cortex	GENE_SYMBOL	GENE_NAME	channel transporter	Metabolic enzymes	cytoskeleton /extracellular matrix
1398612_at	51.8	37.6	1.4	Akr1c12_predicted	aldo-keto reductase family 1, member C12 (predicted)			
1384639_at	51.6	49.0	1.1	Dpl1l_predicted	deleted in polyposis 1-like 1 (predicted)			
1368627_at	49.7	35.7	1.4	Rgn	regucalcin			
1368366_at	47.1	42.1	1.1	Cml2	Camello-like 2			
1387234_at	44.2	42.4	1.0	Azgp1	alpha-2-glycoprotein 1, zinc			
1368163_at	43.3	43.2	1.0	Dpp4	dipeptidylpeptidase 4			
1372841_at	41.7	32.3	1.3	Dpl1l_predicted	deleted in polyposis 1-like 1 (predicted)			
1398255_at	38.7	20.9	1.8	Slc15a2	solute carrier family 15 (H+/peptide transporter), member 2			
1367905_at	38.2	29.7	1.3	Enpp3	ectonucleotide pyrophosphatase/phosphodiesterase 3			
1370688_at	33.0	27.8	1.2	Gclc	glutamate-cysteine ligase, catalytic subunit			
1368374_a_at	31.9	29.2	1.1	Ggt1	gamma-glutamyltransferase 1			
1387218_at	30.2	23.1	1.3	Tff3	trefoil factor 3			
1370714_a_at	30.0	17.1	1.8	Siat1	sialyltransferase 1			
1373773_at	29.4	25.3	1.2	Gpm6a	glycoprotein m6a			
1387357_at	28.1	24.8	1.1	Tmlhe	trimethyllysine hydroxylase, epsilon			
1380962_at	27.6	23.3	1.2	Ace2	Angiotensin I converting enzyme (peptidyl-dipeptidase A) 2			
1370144_at	26.9	18.1	1.5	Gtpbp4 /// LOC364763 /// LOC498786	G protein-binding protein CRFG /// similar to GTP-binding protein NGB /// similar to GTP-binding protein NGB			
1387209_at	24.6	22.3	1.1	Rgpr	regucalcin gene promotor region related protein			
1367838_at	24.5	17.9	1.4	Cth	CTL target antigen			
1390855_at	23.9	12.7	1.9	Prep	Prolyl endopeptidase			
1371913_at	23.4	11.8	2.0	Tgfbi	transforming growth factor, beta induced			
1368234_at	23.4	12.1	1.9	Prep	prolyl endopeptidase			
1388145_at	22.5	22.4	1.0	Tnxa	tenascin XA			
1370365_at	22.3	14.3	1.6	Gss	glutathione synthetase			
1381350_at	20.3	17.4	1.2	Idb4	inhibitor of DNA binding 4			
1394022_at	18.0	11.8	1.5	Idb4	inhibitor of DNA binding 4			
1368164_at	17.9	14.7	1.2	Blvra	biliverdin reductase A			
1379300_at	17.5	17.0	1.0	Chst2_predicted	carbohydrate sulfotransferase 2 (predicted)			
1387296_at	17.1	15.7	1.1	Cyp2j4	cytochrome P450, family 2, subfamily J, polypeptide 4			
1377408_at	16.9	16.2	1.0	Pla2g6	phospholipase A2, group VI			
1369407_at	16.8	10.4	1.6	Tnfrsf11b	tumor necrosis factor receptor superfamily, member 11b (osteoprotegerin)			
1382868_at	16.5	9.9	1.7	Sema6a_predicted	sema domain, transmembrane domain (TM), and cytoplasmic domain, (semaphorin) 6A (predicted)			
1387819_at	16.3	16.3	1.0	Ela1	elastase 1, pancreatic			
1372523_at	16.3	14.9	1.1	Gclc	glutamate-cysteine ligase, catalytic subunit			

Table 4. Continued.

Probe sets	medulla/ papilla	cortex/ papilla	medulla/ cortex	GENE_SYMBOL	GENE_NAME	channel transporter	Metabolic enzymes	cytoskeleton /extracellular matrix
1387941_s_at	16.1	14.6	1.1	Pla2g6	phospholipase A2, group VI			
1372750_at	3.7	0.2	15.9	Fst	Follistatin			
1370072_at	15.6	12.1	1.3	Mme	membrane metallo endopeptidase			
1387966_at	15.5	11.4	1.4	Asrgl1	asparaginase-like sperm autoantigen			
1384831_at	15.1	11.7	1.3	Slc7a13_predicted	solute carrier family 7, (cationic amino acid transporter, y+ system) member 13 (predicted)			
1368189_at	14.8	11.3	1.3	Dhcr7	7-dehydrocholesterol reductase			
1367798_at	14.5	11.2	1.3	Ahcy	S-adenosylhomocysteine hydrolase			
1371059_at	14.5	14.4	1.0	Prkar2a	protein kinase, cAMP-dependent, regulatory, type 2, alpha			
1369158_at	14.4	14.3	1.0	Casr	calcium-sensing receptor			
1370030_at	14.1	11.5	1.2	Gclm	glutamate cysteine ligase, modifier subunit			
1398350_at	14.0	12.9	1.1	Basp1	brain abundant, membrane attached signal protein 1			
1369728_at	13.7	10.7	1.3	Hist1h4m_predicted	histone 1, H4m (predicted)			
1387223_at	13.6	12.2	1.1	Aadat	aminoadipate aminotransferase			
1370529_a_at	12.8	7.7	1.7	Pld1	phospholipase D1			
1384603_at	12.8	9.8	1.3	Abca4_predicted	ATP-binding cassette, sub-family A (ABC1), member 4 (predicted)			
1369494_a_at	12.0	6.6	1.8	Ghrhr	growth hormone releasing hormone receptor			
1367729_at	11.9	11.4	1.0	Oat	ornithine aminotransferase			
1374565_at	11.8	9.7	1.2	Nek6	NIMA (never in mitosis gene a)-related expressed kinase 6			
1368431_at	11.6	10.3	1.1	Hpn	hepsin			
1382274_at	11.5	5.5	2.1	Rarres1_predicted	retinoic acid receptor responder (tazarotene induced) 1 (predicted)			
1374871_at	11.2	7.3	1.5	Asrgl1	asparaginase-like sperm autoantigen			
1392965_a_at	11.0	2.3	4.8	Smoc2_predicted	SPARC related modular calcium binding 2 (predicted)			
1370163_at	11.0	6.5	1.7	Odc1	ornithine decarboxylase 1			
1390208_at	10.7	10.7	1.0	Htatip2_predicted	HIV-1 Tat interactive protein 2 (predicted)			
1370530_a_at	10.6	5.7	1.9	Pld1	phospholipase D1			
1376852_at	10.5	8.3	1.3	Mccc1_predicted	methylcrotonoyl-Coenzyme A carboxylase 1 (alpha) (predicted)			
1369184_at	10.5	6.8	1.5	Cldn16	claudin 16			
1385970_at	10.4	9.5	1.1	Sh2bp1_predicted	SH2 domain binding protein 1 (tetratricopeptide repeat containing) (predicted)			
1383742_at	10.1	9.4	1.1	Snx7_predicted	sorting nexin 7 (predicted)			

After selection by ANOVA ($p<0.01$) for the data of percellome normalization, genes maximally expressed in medulla were selected. The genes were aligned in the order of the ratio to the lower expression value, either in papilla or in cortex. As the genes listed here are expressed in medulla and cortex to a similar extent, exceptional cases (ratio >3) are shaded in the medulla/cortex column. The genes categorized to "channel/transporters", "metabolic enzymes", or "cytoskeleton/extracellular matrix" are also shaded. Proteases or enzymes involving signal transduction are not included in the category of "metabolic enzymes". For simplicity, genes with less than 10-fold specificity are omitted.

Table 5. A list of probe sets specifically expressed in cortex of kidney.

Probe sets	cortex/ papilla	medulla/ papilla	cortex/ medulla	GENE_SYMBOL	GENE_NAME	channel transporter	Metabolic enzymes	cytoskeleton /extracellular matrix
1387314_at	312.0	259.8	1.2	Sult1b1	sulfotransferase family 1B, member 1			
1387820_at	284.9	14.7	19.4	Klk7	kallikrein 7			
1388172_at	245.4	110.3	2.2	Ust1r	integral membrane transport UST1r			
1368064_a_at	230.1	19.6	11.8	Ddc	dopa decarboxylase			
1390591_at	224.2	166.1	1.3	Slc17a3	Na/Pi cotransporter 4			
1368467_at	217.1	117.6	1.8	Cyp4f2	cytochrome P450, family 4, subfamily F, polypeptide 2			
1368600_at	210.7	75.0	2.8	Slc26a1	solute carrier family 26 (sulfate transporter), member 1			
1396039_at	202.5	188.6	1.1	Slc22a12_predicted	solute carrier family 22 (organic anion/cation transporter), member 12 (predicted)			
1387230_at	193.9	13.2	14.7	Slc12a3	solute carrier family 12, member 3			
1368245_at	192.4	134.7	1.4	Upb1	ureidopropionase, beta			
1367917_at	192.3	124.6	1.5	Cyp2d26	cytochrome P450, family 2, subfamily d, polypeptide 26			
1367871_at	187.8	32.3	5.8	Cyp2e1	cytochrome P450, family 2, subfamily e, polypeptide 1			
1376267_at	185.1	13.9	13.4	Slc16a6	Solute carrier family 16 (monocarboxylic acid transporters), member 6			
1384877_at	183.4	73.9	2.5	Aqp11	aquaporin 11			
1398282_at	174.5	75.2	2.3	Kynu	kynureninase (L-kynurenine hydrolase)			
1370547_at	169.5	56.4	3.0	Pzp	pregnancy-zone protein			
1368563_at	149.7	96.7	1.5	Aspa	aspartoacylase			
1383111_at	149.3	60.1	2.5	Acmsd	2-amino-3-carboxymuconate-6-semialdehyde decarboxylase			
1370991_at	146.7	32.6	4.5	Cml3	camello-like 3			
1387188_at	144.5	86.8	1.7	RGD:620099	solute carrier family 17 (sodium phosphate), member 1			
1370936_at	143.4	91.3	1.6	Dmgdh	dimethylglycine dehydrogenase precursor			
1367804_at	142.8	21.8	6.5	Sap	serum amyloid P-component			
1368915_at	141.5	87.2	1.6	Kmo	kynurenine 3-monooxygenase (kynurenine 3-hydroxylase)			
1398511_at	138.7	16.8	8.3	Susd2_predicted	sushi domain containing 2 (predicted)			
1387851_at	129.9	78.3	1.7	Pter	phosphotriesterase related			
1376051_at	127.0	63.2	2.0	Cryl1	crystallin, lamda 1			
1384112_at	125.1	80.6	1.6	Nt5	5 nucleotidase			
1393894_at	123.8	94.1	1.3	RGD:628846	cytochrome P450, 4a12			
1370725_a_at	116.9	15.4	7.6	G6pc	glucose-6-phosphatase, catalytic			
1386980_at	116.6	64.2	1.8	Apom	apolipoprotein M			
1377125_at	116.3	28.0	4.2	Dnajc6_predicted	DnaJ (Hsp40) homolog, subfamily C, member 6 (predicted)			
1368317_at	114.8	70.5	1.6	Aqp7	aquaporin 7			
1370615_at	114.4	28.0	4.1	RGD:708417	UDP-glucuronosyltransferase			

Table 5. Continued.

Probe sets	cortex/ papilla	medulla/ papilla	cortex/ medulla	GENE_SYMBOL	GENE_NAME	channel transporter	Metabolic enzymes	cytoskeleton /extracellular matrix
1368236_at	113.4	105.5	1.1	Mep1a	meprin 1 alpha			
1373386_at	113.2	110.8	1.0	Gjb2	gap junction membrane channel protein beta 2			
1369636_at	112.6	41.2	2.7	Sord	sorbitol dehydrogenase			
1368521_at	110.8	46.3	2.4	Napsa	napsin A aspartic peptidase			
1368150_at	110.4	78.2	1.4	Slc27a2 /// LOC497779	solute carrier family 27 (fatty acid transporter), member 2 /// hypothetical gene supported by NM_031736			
1369635_at	109.5	42.4	2.6	Sord	sorbitol dehydrogenase			
1368180_s_at	107.9	73.9	1.5	Gsta2	glutathione-S-transferase, alpha type2			
1368190_at	105.6	12.1	8.7	Ren1	renin 1			
1377051_at	104.7	17.9	5.8	Mpv17l_predicted	Mpv17 transgene, kidney disease mutant-like (predicted)			
1387336_at	102.7	89.7	1.1	Nat8	*N*-acetyltransferase 8 (camello like)			
1387631_at	102.4	59.8	1.7	Hpgd	15-hydroxyprostaglandin dehydrogenase			
1379885_at	100.7	91.4	1.1	Fmo4	flavin containing monooxygenase 4			
1368659_at	100.0	60.0	1.7	Agxt2	alanine-glyoxylate aminotransferase 2			
1370259_a_at	99.6	31.1	3.2	Pthr1	parathyroid hormone receptor 1			
1368188_at	94.6	25.6	3.7	Hpd	4-hydroxyphenylpyruvic acid dioxygenase			
1369200_at	93.4	56.3	1.7	Nt5	5 nucleotidase			
1387053_at	90.3	37.7	2.4	Fmo1	flavin containing monooxygenase 1			
1388569_at	88.3	50.7	1.7	Serpinf1	serine (or cysteine) proteinase inhibitor, clade F), member 1			
1390857_at	87.5	26.6	3.3	Xylb_predicted	xylulokinase homolog (H. influenzae) (predicted)			
1387375_at	86.9	64.4	1.4	Khk	ketohexokinase			
1387034_at	86.3	17.7	4.9	Pah	phenylalanine hydroxylase			
1397740_at	86.3	51.0	1.7	Sfxn1_predicted	sideroflexin 1 (predicted)			
1368736_at	84.2	18.9	4.4	Tsx	testis specific X-linked gene			
1398514_at	82.6	81.3	1.0	Hgd_predicted	homogentisate 1, 2-dioxygenase (predicted)			
1368515_at	81.1	7.2	11.3	Epb4.1l3	erythrocyte protein band 4.1-like 3			
1368794_at	81.0	78.4	1.0	Haao	3-hydroxyanthranilate 3,4-dioxygenase			
1370964_at	80.8	27.0	3.0	Ass	arginosuccinate synthetase			
1368077_at	79.6	43.0	1.9	Fbp1	fructose-1,6- biphosphatase 1			
1370397_at	77.6	68.8	1.1	Cyp4a14	cytochrome P450, family 4, subfamily a, polypeptide 14			
1368397_at	76.3	36.6	2.1	Ugt2b5 /// Ugt2b4	UDP-glucuronosyltransferase 2 family, member 5 /// UDP glycosyltransferase 2 family, polypeptide B4			
1368282_at	74.3	24.9	3.0	Dpep1	dipeptidase 1 (renal)			
1395026_at	73.7	59.0	1.2	Fmo4	flavin containing monooxygenase 4			
1380577_at	70.1	53.6	1.3	Abcg2	ATP-binding cassette, sub-family G (WHITE), member 2			

Table 5. Continued.

Probe sets	cortex/ papilla	medulla/ papilla	cortex/ medulla	GENE_SYMBOL	GENE_NAME	channel transporter	Metabolic enzymes	cytoskeleton /extracellular matrix
1387339_at	69.4	19.2	3.6	Sepp1	selenoprotein P, plasma, 1			
1382913_at	68.9	16.8	4.1	Cttnbp2	cortactin binding protein 2			
1376327_at	68.9	24.2	2.8	Tnfrsf14_predicted	tumor necrosis factor receptor superfamily, member 14 (herpesvirus entry mediator) (predicted)			
1368178_at	66.6	32.4	2.1	Pdzk1	PDZ domain containing 1			
1377672_at	66.3	37.3	1.8	Sult1c2	sulfotransferase family, cytosolic, 1C, member 2			
1387084_at	65.5	55.5	1.2	Dpp4	dipeptidylpeptidase 4			
1374512_at	63.7	35.5	1.8	Cdh7	Cadherin 7, type 2			
1371824_at	63.6	40.8	1.6	Ak3l1	adenylate kinase 3-like 1			
1369412_a_at	63.4	37.9	1.7	Slc19a1	solute carrier family 19, member 1			
1373803_a_at	63.1	39.2	1.6	Ghr	growth hormone receptor			
1387259_at	62.9	29.4	2.1	Cdh2 /// LOC497718	cadherin 2 /// hypothetical gene supported by NM_031333			
1389166_at	62.8	31.1	2.0	Cib2_predicted	calcium and integrin binding family member 2 (predicted)			
1371354_at	62.1	8.0	7.8	Tncc_predicted	troponin C, cardiac/slow skeletal (predicted)			
1372672_at	58.8	36.8	1.6	Qprt_predicted	quinolinate phosphoribosyltransferase (predicted)			
1369491_at	58.4	36.1	1.6	Dao1	D-amino acid oxidase			
1387111_at	57.3	33.4	1.7	Ddah1	dimethylarginine dimethylaminohydrolase 1			
1367988_at	57.1	22.1	2.6	Cyp2c23	cytochrome P450, family 2, subfamily c, polypeptide 23			
1368607_at	56.5	51.1	1.1	RGD:628846	cytochrome P450, 4a12			
1370881_at	55.8	22.9	2.4	Tst	thiosulfate sulfurtransferase			
1369259_at	55.6	28.4	2.0	Dio1	deiodinase, iodothyronine, type I			
1376709_at	55.2	42.5	1.3	Slc39a8_predicted	solute carrier family 39 (metal ion transporter), member 8 (predicted)			
1387013_at	55.2	27.3	2.0	Tmem27	kidney-specific membrane protein			
1387808_at	54.9	5.1	10.8	Slc7a7	solute carrier family 7 (cationic amino acid transporter, y+ system), member 7			
1368283_at	54.7	29.8	1.8	Ehhadh	enoyl-Coenzyme A, hydratase/3-hydroxyacyl Coenzyme A dehydrogenase			
1373337_at	53.4	22.5	2.4	Grhpr_predicted	glyoxylate reductase/hydroxypyruvate reductase (predicted)			
1383654_a_at	53.2	14.7	3.6	Fnsk	similar to fructosamine-3-kinase			
1368924_at	51.8	42.4	1.2	Ghr	growth hormone receptor			
1368092_at	50.7	35.9	1.4	Fah	fumarylacetoacetate hydrolase			
1380171_at	49.4	39.5	1.3	Adra2b	Adrenergic receptor, alpha 2b			
1367952_at	45.8	26.5	1.7	Lrp2	low density lipoprotein receptor-related protein 2			

Table 5. Continued.

Probe sets	cortex/ papilla	medulla/ papilla	cortex/ medulla	GENE_SYMBOL	GENE_NAME	channel transporter	Metabolic enzymes	cytoskeleton /extracellular matrix
1369705_at	44.1	42.6	1.0	RGD:621651	X transporter protein 3			
1368680_a_at	43.6	25.3	1.7	Slc34a1	solute carrier family 34 (sodium phosphate), member 1			
1367627_at	43.5	14.8	2.9	Gatm	glycine amidinotransferase (L-arginine:glycine amidinotransferase)			
1379950_at	42.9	37.7	1.1	Cml2	Camello-like 2			
1367775_at	42.6	32.3	1.3	Amacr	alpha-methylacyl-CoA racemase			
1388176_at	42.4	24.0	1.8	Cml5	camello-like 5			
1368322_at	42.1	8.2	5.1	Sod3	superoxide dismutase 3, extracellular			
1372264_at	42.1	15.9	2.7	Pck1	phosphoenolpyruvate carboxykinase 1			
1397647_at	41.9	17.1	2.5	Slc25a15_predicted	solute carrier family 25 (mitochondrial carrier; ornithine transporter) member 15 (predicted)			
1369073_at	41.9	12.2	3.4	Nr1h4	nuclear receptor subfamily 1, group H, member 4			
1368877_at	41.6	13.7	3.0	Znf354a	zinc finger protein 354A			
1390119_at	41.4	4.9	8.4	Sfrp2	secreted frizzled-related protein 2			
1367774_at	41.1	31.8	1.3	Gsta5	glutathione S-transferase A5			
1376191_at	40.1	27.6	1.5	Hpgd	15-hydroxyprostaglandin dehydrogenase			
1397526_at	39.3	23.5	1.7	Gcdh_predicted	glutaryl-Coenzyme A dehydrogenase (predicted)			
1374384_at	38.8	16.3	2.4	Crygc	Crystallin, gamma C			
1387491_at	38.5	10.9	3.5	Gyk	glycerol kinase			
1386944_a_at	38.3	7.7	5.0	G6pc	glucose-6-phosphatase, catalytic			
1367999_at	37.7	22.6	1.7	Aldh2	aldehyde dehydrogenase 2			
1369182_at	37.6	9.6	3.9	F3	coagulation factor 3			
1382975_at	37.4	20.8	1.8	Ceacam1	CEA-related cell adhesion molecule 1			
1374200_at	36.1	16.7	2.2	Slc29a3	solute carrier family 29 (nucleoside transporters), member 3			
1369973_at	35.6	9.6	3.7	Xdh /// LOC497811	xanthine dehydrogenase /// hypothetical gene supported by NM_017154			
1372306_at	35.4	22.9	1.5	Ethe1_predicted	ethylmalonic encephalopathy 1 (predicted)			
1370818_at	34.6	12.5	2.8	Decr2	2-4-dienoyl-Coenzyme A reductase 2, peroxisomal			
1397797_at	33.3	29.3	1.1	Tigd3	Tigger transposable element derived 3 (predicted)			
1372323_at	32.9	23.4	1.4	Sardh	sarcosine dehydrogenase			
1368412_a_at	32.5	5.3	6.1	Ptpro	protein tyrosine phosphatase, receptor type, O			
1390036_at	32.5	6.0	5.4	Slc16a6	solute carrier family 16 (monocarboxylic acid transporters), member 6			
1397744_at	32.5	22.2	1.5	Sardh	Sarcosine dehydrogenase			
1368642_at	32.4	19.5	1.7	Cdh2 /// LOC497718	cadherin 2 /// hypothetical gene supported by NM_031333			
1373188_at	32.0	12.2	2.6	Scn4b	sodium channel, voltage-gated, type IV, beta			

Table 5. Continued.

Probe sets	cortex/ papilla	medulla/ papilla	cortex/ medulla	GENE_SYMBOL	GENE_NAME	channel transporter	Metabolic enzymes	cytoskeleton /extracellular matrix
1373667_at	31.8	14.0	2.3	Ccbl1_predicted	cysteine conjugate-beta lyase (predicted)			
1372031_at	31.7	7.5	4.2	Dab2	Disabled homolog 2 (Drosophila)			
1390585_at	31.7	10.9	2.9	Masp1	mannan-binding lectin serine peptidase 1			
1386981_at	31.6	3.7	8.4	Slc16a1	solute carrier family 16 (monocarboxylic acid transporters), member 1			
1368253_at	31.5	28.7	1.1	Gamt	guanidinoacetate methyltransferase			
1388537_at	31.4	15.2	2.1	Nipsnap1_predicted	4-nitrophenylphosphatase domain and non-neuronal SNAP25-like protein homolog 1 (C. elegans) (predicted)			
1387165_at	31.1	4.4	7.1	Maf	v-maf musculoaponeurotic fibrosarcoma (avian) oncogene homolog (c-maf)			
1384273_at	30.9	10.2	3.0	Carkl_predicted	carbohydrate kinase-like (predicted)			
1380393_at	30.9	30.7	1.0	Cryz_predicted	crystallin, zeta (predicted)			
1393947_at	30.7	12.7	2.4	Slc25a15_predicted	solute carrier family 25 (mitochondrial carrier; ornithine transporter) member 15 (predicted)			
1378197_at	30.4	9.5	3.2	KIFC2	kinesin family member C2			
1379582_a_at	30.1	14.5	2.1	Ccna2	cyclin A2			
1382434_at	30.0	23.5	1.3	Entpd5	ectonucleoside triphosphate diphosphohydrolase 5			

After selection by ANOVA ($p<0.01$) for the data of percellome normalization, genes maximally expressed in cortex were selected. The genes were aligned in the order of the ratio to the lower expression value, either in papilla or in medulla. Among the genes listed here, relatively specific ones for cortex (ratio>3) are shaded in the cortex/medulla column. The genes categorized to "channel/transporters", "metabolic enzymes", or "cytoskeleton/extracellular matrix" are also shaded. Proteases or enzymes involving signal transduction are not included in the category of "metabolic enzymes". For simplicity, genes with less than 30-fold specificity are omitted.

Table 6. Regionally specific genes in rat kidney.

	Channel/transporter	Metabolizing enzymes	Cytoskeleton/ extracellular matrix	Others of interest
Papilla	Slco4a1, Aqp3, Aqp4, Fxyd4, Slc4a11, Clcnk1, bsnd	Ptgs1, Ptgs2, Aldh1a3, Akr1b4, Ugt8, Ltb4dh	Capg, Plekhb1, Col18a1, Spnb3, Hs3st1, Krt1-18	Hspa2, Hspa1a, Hspb1
Medulla	Scl21a1, Scl21a13, Slc23a3, Slc21a9, UST5r, Scl6a18, Scl38a3, Slc22a2, Slc7a12, Slc15a2	CYP2d9, CYP2c, Hnmt, Pklr, Fmo3, Dhrs7, Akr1c12, Gclc, Ggt1, Tmlhe		Prlr, Ace2
Cortex	Ust1r, Slc17a3, Slc26a1, Slc22a12, Slc12a3, Slc16a6, Aqp11, Aqp7, Gjb2, Slc27a2	Sult1b1, Klk7, Ddc, CYP2d26, CYP2e1, CYP4f2, Upb1, Aspa, Acmsd, Dmgdh, Kmo		Ren1

Genes categorized in channel/transporter, metabolizing enzyme and cytoskeleton/extracellular matrix from high rank in Tables 3, 4, 5 are summarized by using gene symbols which can be referred to in the preceding tables. Interesting genes discussed in the text are included as "others".

aminoglycoside causes necrosis mainly in the proximal tubules, while puromycin does the same on glomerulus (Schnellmann, 2001). In an organ with such a complex structure, analysis by GeneChip would give different results when it is done as a whole or separated into portions. When the potential nephrotoxicity of candidate chemicals is assessed using toxicogenomics technology, it would be ideal to perform GeneChip analysis for each portion. However, it is sometimes difficult in the usual toxicity tests to obtain enough sample material for toxicogenomics analysis after sampling for other histopathological and biochemical analyses. Furthermore, it is difficult to determine which portion is to be examined when the target region of the test drug is unknown. Analyzing all of the separated portions is impractical considering the cost.

In the present study, comparison of the gene expression profile was made among each portion, papilla, medulla, and cortex, as well as between the whole slice and each portion. Although various genes or proteins with region-specific expression have been reported, their localization was toward glomerulus, distal/proximal tubules, or collecting duct, i.e., tissues from specific cell types, not the anatomical location. This way is of course desirable for cell physiological study, but is inconvenient when a potential bias in the gene expression analysis based on the position of sampling is concerned, and reports focusing on this point are scarce. It can be generally said that papilla is enriched in collecting duct and relatively scarce in glomerulus, but their proportion varies with the sampling.

When comparison between each portion was made by correlation coefficient, the correlation was decreased between the portions compared to within the same portion. The correlation of gene expression profile between cortex and medulla was relatively high, whereas that between papilla and cortex or medulla was low. Based on the correlation of each portion to the whole slice, it was concluded that gene expression in the whole slice largely reflected that of cortex, followed by medulla. The main reason is that the volume of the portion comprising the whole slice is in this order: cortex > medulla > papilla (Fig. 1). If the production of mRNA per cell is constant throughout the portions, the region-specific gene can be extracted by global normalization. However, this was found to be inappropriate.

To extract region-specific genes, detection call (absent, present, and marginal) included in the GeneChip data was utilized, i.e., genes with present call in a particular region but absent call in all others were extracted, and they were checked as to whether they had present call in the whole slice. The important point of this result is that the majority (94%) of genes specifically expressed in papilla are not detectable in the whole slice. This is consistent with the result of the correlation coefficient. It is thus concluded that the expression changes of such genes occurring in papilla cannot be detected when they are decreased, and it is difficult to measure when they are increased, but their extent is not so large, as in the analysis of the whole slice. Attention should be paid when these genes are used for the marker genes in the toxicogenomics of kidney.

As obvious from Figs. 3 and 4, global normalization of the data leads to an incorrect result in the comparison among different regions. This might be due to the fact that the transcriptional activity in papilla is much less than that in the others, and subsequently the expression of each gene in papilla was over-estimated by the normalization, using a low value. This does not mean that the global normalization is useless when drug effects are tested on the samples separated into different portions. As global normalization gives relative values to the total mRNA amount, it efficiently reveals the drug effect unless the drug brings about a large change in the total mRNA. In the present case, it became problematic simply because the comparison was made among tissues with largely different mRNA contents. An alternative way is to normalize each gene by a house-keeping gene, e.g., β-actin or GAPDH. However, as already shown above, there is no guarantee that expression of these genes is constant throughout the different tissues.

Based on the data normalized by the percellome procedure, genes with region-specific expression were extracted and aligned in the order of their relative specificity. It was then found that the majority of genes with high region-specificity were related to channel/transporter and metabolic enzyme, suggesting a good correlation between gene expression and physiological function.

There are many known members of the solute carrier family (slc), whose distribution showed an interesting and marked difference among the three portions. In papilla, slc4a family members (anion transporter) were specifically expressed. In medulla, the expression of slc21a family (organic anion transporting polypeptides; OATPs), was outstanding. There were also other members such as Slc23a3 (xanthine/uracil permease), Scl6a18 (monocarboxylic acid trans-

porter), Scl38a3 (SNAT family; Gu *et al.*, 2005), Slc22a2 (organic cation transporter), Slc7a12 (cationic amino acid transporter), and Slc15a2 (H+/peptide transporter), which were specifically expressed. In cortex, Slc17a (Na-phosphate co-transporter), Slc22a12 and Slc12a3 (both anion transporters), Slc16a6 (monocarboxylic acid transporter), and Slc27a2 (fatty acid transporter) were found to be specific.

There have been some reports regarding region-specific transporters. As glucose transport is known to be operational in the proximal tubule, it is expected that glucose transporters are enriched in cortex and medulla compared with papilla. Among the genes judged as significant by ANOVA, slc2a4 and 2a13 were glucose transporters and their expression was about 3.5-fold higher in medulla and cortex compared with papilla (this number was not large enough to be shown in the tables). It is also known that slc14a2, involved in urea transport, is highly expressed in the collecting duct (Karakashian *et al.*, 1999). Although the ratio was not large enough to be in Table 3, its expression in papilla was twofold compared with cortex, consistent with the literature.

Aquaporin (Aqp) 3 and 4 were specifically expressed in papilla while Aqp 7 and 11 were in cortex (Table 6). Although the ratio was not large enough to be in Table 3, Aqp 2 was also preferentially expressed in papilla (1.9 and 2.3 fold compared with medulla and cortex, respectively). There have been supportive reports that Aqp2 (Jo *et al.*, 1997) and Aqp3 (Echevarria *et al.*, 1994) are enriched in collecting duct and Aqp7 is highly expressed in cortex (Nejsum *et al.*, 2000).

Kidney produces renin to control blood pressure. Renin is synthesized in juxtaglomerular cells and converts angiotensinogen to angiotensin I, which is further converted to angiotensin II by angiotensin converting enzyme (ACE). The renin gene (Ren1) was expressed highest in cortex while ACE (ace2) was highest in medulla (Table 6).

Probes for prolactin receptor are 4 sets on the chip and all of them showed quite low expression in papilla (expression ranged 60 - 90 fold in cortex and 70 - 130 fold in medulla, compared with papilla, for these 4 probe sets). Prolactin is known as a natriuretic hormone which interacts with the renal dopamine system, and its natriuretic response is associated with inhibition of proximal tubular Na,K-ATPase (Ibarra *et al.*, 2005). The location of its receptor in kidney (enriched in medulla and cortex) elucidated in the present study was consistent with the region where the hormone works.

NSAID-induced nephrotoxicity is well known as a typical toxicity toward kidney (Schnellmann, 2001). Its mechanism is believed to be inhibition of cyclooxygenase (COX). COX-1 is a constitutive, house-keeping enzyme and reported to be much present in the collecting duct. COX-2 is an inducible enzyme involved in the inflammatory process, while it is reported to be always present at a low level in kidney without inflammation (Harris *et al.*, 1994). The genes for these enzymes (ptgs1 and ptgs2) were both highest in papilla. Moreover, phospholipase A2 IVA was also highest in papilla. These observations are consistent with previous reports and might be related to the fact that nephrotoxicity by NSAID is frequently associated with necrosis in papilla (Schnellmann, 2001).

On the other hand, other prostaglandin-related genes were uniformly low in papilla. The expression of the gene of 15-hydroxyprostaglandin dehydrogenase (Hpgd), which is involved in prostaglandin metabolism, was 60 and 102 fold in medulla and cortex, respectively, compared with papilla. Other prostaglandin-related genes without large enough specificity for the table were prostaglandin D2 synthase (Ptgds), prostaglandin E receptor 1 (Ptger1), prostaglandin E receptor 3 (Ptger3), and prostaglandin E receptor 4 (Ptger4), which were 6- and 26-fold, 3- and 4-fold, 5- and 2-fold, 3- and 6-fold, in medulla and cortex, respectively, compared with papilla. The expression of prostaglandin E synthase (Ptges) was exceptionally the same in papilla and medulla, and 4.5-fold of these was found in cortex.

Kallikrein that produces bradykinin is biosynthesized in kidney cortex (Xiong *et al.*, 1989). Kallikrein 7 (Klk7) is found in Table 5 showing 15-fold and 285-fold expression in medulla and cortex, respectively, compared with papilla. This is again consistent with the anatomical feature.

One unique point in the tables is that genes related to cytoskeletal proteins and heat shock proteins (both HSP70 and HSP27) selectively expressed high in papilla (Table 3 and 6). If the analysis was done by global normalization, it could be that the relative expression of these genes was apparently overestimated because of the low expression of other gene populations, such as transporters or enzymes. However, the present analysis was based on percellome normalization, and the values are directly related to the copy numbers per cell (or DNA). Therefore, enrichment of these genes means that the copy numbers of these genes are actually high. The potential involvement of

HSP70 in nephrotoxicity has been investigated in relation to renal cell survival and apoptosis, and the relationship between hsp27 and cytoskeletal proteins has also been discussed in relation to renal injury after ischemia-reperfusion (van de Water, 2006). Its pathophysiological meaning is presently unclear, especially because data of modulation by nephrotoxicants is not available, so this point is quite interesting as a future study.

In summary, many of the genes related to kidney functions showed region-related differences in their expression and some of them were consistent with previous reports. There are also many genes with unique region-related differences in the table, which have not been described in the literature and it would be worthwhile to start new investigations based on these data. In the present study, analysis of gene expression was exclusively done in non-treated animals. It is of course important to investigate the regional difference in the responsiveness to drugs, and it should be the highest priority of future study. In conclusion, comprehensive comparison data of gene expression in the renal anatomical areas would greatly enhance studies of physiological function and mechanism of toxicity in kidney.

ACKNOWLEDGMENT

This study was supported in part by a grant from the Ministry of Health, Labor and Welfare (H14-Tox-ico-001).

REFERENCES

Echevarria, M., Windhager, E.E., Tate, S.S. and Frindt, G. (1994): Cloning and expression of AQP3, a water channel from the medullary collecting duct of rat kidney. Proc. Natl. Acad. Sci. USA, **91**, 10997-11001.

Gu, S., Villegas, C.J. and Jiang, J.X. (2005): Differential Regulation of Amino Acid Transporter SNAT3 by Insulin in Hepatocytes. J. Biol. Chem., **280**, 26055-26062.

Harris, R.C., McKanna, J.A., Akai, Y., Jacobson, H.R., Dubois, R.N. and Breyer, M.D. (1994): Cyclooxygenase-2 is associated with the macula densa of rat kidney and increases with salt restriction. J. Clin. Invest., **94**, 2504-2510.

Ibarra, F., Crambert, S., Eklof, A.C., Lundquist, A., Hansell, P. and Holtback, U. (2005): Prolactin, a natriuretic hormone, interacting with the renal dopamine system. Kidney Int., **68**, 1700-1707.

Jo, I., Nielsen, S. and Harris, H.W. (1997): The 17 kDa band identified by multiple anti-aquaporin 2 antisera in rat kidney medulla is a histone. Biochim. Biophys. Acta., **1324**, 91-101.

Kanno, J., Aisaki, K., Igarashi, K., Nakatsu, N., Ono, A., Kodama, Y. and Nagao, T. (2006): "Per cell" normalization method for mRNA measurement by quantitative PCR and microarrays. BMC Genomics, **7**, 64.

Karakashian, A., Timmer, R.T., Klein, J.D., Gunn, R.B., Sands, J.M. and Bagnasco, S.M. (1999): Cloning and characterization of two new isoforms of the rat kidney urea transporter: UT-A3 and UT-A4. J. Am. Soc. Nephrol., **10**, 230-237.

Nejsum, L.N., Elkjaer, M., Hager, H., Frokiaer, J., Kwon, T.H. and Nielsen, S. (2000): Localization of aquaporin-7 in rat and mouse kidney using RT-PCR, immunoblotting, and immunocytochemistry. Biochem. Biophys. Res. Commun., **277**, 164-170.

Schnellmann, R.G. (2001): Toxic responses of the kidney. In Casarett & Doull's Toxicology, 6th ed.(Klaassen, C.D., ed.), pp.491-514. McGraw-Hill.

Snedecor, G.W. and Cochran, W.G. (1989): Statistical Methods, 8th ed., Iowa State University Press.

Thukral, S.K., Nordone, P.J., Hu, R., Sullivan, L., Galambos, E., Fitzpatrick, V.D., Healy, L., Bass, M.B., Cosenza, M.E. and Afshari, C.A. (2005): Prediction of nephrotoxicant action and identification of candidate toxicity-related biomarkers. Toxicol. Pathol., **33**, 343-355.

Urushidani, T. and Nagao, T. (2005): Toxicogenomics: The Japanese initiative. In Handbook of Toxicogenomics - Strategies and Applications (Borlak, J., ed.), pp. 623-631. Wiley – VCH.

van de Water, B., de Graauw, M., Le Devedec, S. and Alderliesten, M. (2006): Cellular stress responses and molecular mechanisms of nephrotoxicity. Toxicol. Lett., **162**, 83-93.

Xiong, W., Chao, L. and Chao, J. (1989): Renal kallikrein mRNA localization by in situ hybridization. Kidney Int., **35**, 1324-1329.

The Journal of Toxicological Sciences,
Vol.31, No.5, 471-490, 2006

PROFILING OF GENE EXPRESSION IN RAT LIVER AND RAT PRIMARY CULTURED HEPATOCYTES TREATED WITH PEROXISOME PROLIFERATORS

Kotaro TAMURA[1], Atsushi ONO[1], Toshikazu MIYAGISHIMA[1], Taku NAGAO[2] and Tetsuro URUSHIDANI[1,3]

[1]*Toxicogenomics Project, National Institute of Biomedical Innovation, 7-6-8 Saito-Asagi, Ibaraki, Osaka 567-0085, Japan*

[2]*National Institute of Health Sciences, 1-18-1 Kamiyoga, Setagaya-Ku, Tokyo 158-8501, Japan*

[3]*Department of Pathophysiology, Faculty of Pharmaceutical Sciences, Doshisha Women's College of Liberal Arts, Kodo, Kyotanabe, Kyoto 610-0395, Japan*

(Received August 18, 2006; Accepted September 11, 2006)

ABSTRACT — The Toxicogenomics project has been constructing a large-scale database of about 150 compounds exposed to rat (single dose, 3, 6, 9, 24 hrs and repeated dose for 3, 7, 14 28 days with 3 dose levels) and rat hepatocytes (2, 8, 24 hr with 3 concentrations) and data of transcriptome in liver using GeneChip, and the related toxicological measures are being accumulated. In the present study, the data of three ligands of peroxisome proliferator activated receptor α (PPARα), i.e., clofibrate, WY-14643 and gemfibrozil in our database were analyzed. Many of the β-oxidation-related genes were commonly induced *in vivo* and *in vitro*, whereas expression changes in genes related to cell proliferation, apoptosis, were detected *in vivo* (single and repeated dose) but not *in vitro*. Changes in those related to the immune response, coagulation and the stress response were also detectable exclusively *in vivo*. Using the genes mobilized in two or three PPARα agonists, hierarchical clustering was performed on 32 compounds stored in our database. In the profiling of an *in vivo* single dose, benzbromarone and aspirin were located in the same cluster of the three PPARα agonists. The clustering of *in vitro* data revealed that benzbromarone, three NSAIDs (aspirin, indomethacin and diclofenac sodium) and valproic acid belonged to the same cluster of PPARα agonists, supporting the reports that benzbromarone,valproic acid and some NSAIDs were reported to be PPARα agonists. Using the genes commonly up-regulated both *in vivo* and *in vitro*, principal component analysis was performed in 32 compounds, and principal component 1 was found to be the convenient parameter to extract PPARα agonist-like compounds from the database.

KEY WORDS: Toxicogenomics, Hepatotoxicity, Peroxisome proliferator

INTRODUCTION

The Toxicogenomics Project is a 5-year collaborative project conducted by the National Institute of Health Sciences (NIHS) and 17 pharmaceutical companies in Japan which started in 2002 (Urushidani and Nagao, 2005). In April 2005, some rearrangements were made and now the project is conducted by NIHS, the National Institute of Biomedical Innovation, and 15 pharmaceutical companies. Its aim is to construct a large-scale toxicology database of transcriptome for prediction of toxicity of new chemical entities in the early stage of drug development. About 150 chemicals, mainly medicinal compounds, have been selected, and the following are examined for each. The *in vivo* test using rats consists of a single administration test (3, 6, 9 and 24 hr with 4 dose levels including vehicle control) as well as a repeated administration test (3, 7, 14

Correspondence: Tetsuro URUSHIDANI (E-mail: turushid@dwc.doshisha.ac.jp)

and 28 days with 4 dose levels including vehicle control) and the data of body weight, general symptoms, histopathological examination of liver and kidney, and blood biochemistry are obtained from each animal. The gene expression in liver (kidney in some cases) is comprehensively analyzed using Affymetrix GeneChip. An *in vitro* test using rat and human hepatocytes is also carried out to accomplish the bridging between the species. By the time the present study was performed, more than 100 chemicals covering wide medication categories had been finished or were ongoing, and the whole data set of 32 compounds had been stored in the database ready for analysis. We have started the analysis with three fibric acids in the database, i.e., clofibrate, WY-14643 and gemfibrozil (ligands of peroxisome proliferator-activated receptor α, PPARα). They have been extensively studied regarding their mechanism of toxicity, as we consider them excellent model cases for evaluating the quality of our database.

MATERIALS AND METHODS

Compounds

All compounds were of the highest grade obtainable from the suppliers listed in Table 1.

In vivo studies

Male Sprague-Dawley rats were purchased from Charles River Japan Inc., (Kanagawa, Japan) at 5-weeks of age. After a 7-day quarantine and acclimatization period, the animals were divided into groups of 5 animals using a computerized stratified random grouping method based on body weight for each age. The animals were individually housed in stainless-steel cages on a 12 hr light/dark cycle. Each animal was allowed free access to water and pellet food (CRF-1, sterilized by radiation, Oriental Yeast Co., Japan). The test compounds were suspended in 0.5% methylcellulose solution or corn oil. Animals were orally administered daily at three dose levels for 1, 3, 7, 14 and 28 days. The highest dose level for each was determined in a 1-week dose-finding study (data not shown), and 1/3 and 1/10 of that were set as middle and low doses, respectively. The dose levels are given in Table 1.

Blood samples were taken at 3, 6, 9, and 24 hr after single dosing and 24 hr after repeated dosing with a needle and a heparinized syringe from the abdominal artery of animals under ether anesthesia. Plasma biochemical assessments were conducted by using COBAS MIRA plus autoanalyzer (Roche Diagnostics, Basel, SZ). After collecting the blood, the animals were euthanized by exsanguination from the abdominal veins and arteries under ether anesthesia. Livers were collected from each animal and weighed, then a portion (about 30 mg) of each left lateral lobe was put into RNAlater® (Ambion, Austin, TX, USA) for expression profiling. The remaining liver samples were fixed in 10% buffered formalin solution for routine histological processing. Paraffin sections were stained with hematoxylin and eosin for histopathological examination. The experimental protocols were reviewed and approved by the Ethics Review Committee for Animal Experimentation of the National Institute of Health Sciences.

In vitro studies

Hepatocytes were isolated from 6-week-old male Sprague-Dawley rats under sodium pentobarbital (120 mg/kg, ip) by a modified two-step collagenase perfusion method. The liver was perfused via the portal vein for 10 min with divalent cation-free EGTA (0.5 mM)-supplemented HEPES buffered Hank's balanced salt solution followed by a 10-min perfusion with HEPES-buffered normal Hank's balanced salt solution containing soybean trypsin inhibitor (Sigma, T-2011, 0.05 g/L) and collagenase (WAKO 034-10533, 0.5 g/L) at a flow rate of 10 - 30 ml/min. Isolated cells were washed three times by 50 g for 1 min to obtain a parenchymal cell-enriched pellet. Hepatocytes were not used when their viability assessed by trypan blue exclusion was lower than 70%. The cells were seeded into collagen-coated six-well plates (BD BioCoat® Collagen I Cellware, BD Bioscience) at a density of 1×10^6 cells/well in 2 ml HMC Bulletkit medium (CAMBREX) supplemented with 10% fetal bovine serum. Following an attachment period of 3 hr, the medium was replaced and kept overnight before drug exposure at 37°C in an atmosphere of 5% CO_2. The test compounds were added to the medium directly or as a 1,000× stock solution in dimethylsulfoxide. The highest concentration of each compound was determined in a pilot test based on cytotoxicity (ca. 20% release of lactate dehydrogenase) and 1/5 and 1/25 of that were set as middle and lowest concentrations (data not shown). After 2, 8 and 24 hr-exposure, the cells were dissolved with RLT buffer (Qiagen) and collected for expression profiling. GeneChip® analysis was performed in a duplicated manner for each time and concentration point.

Expression profiling

The livers were homogenized using Mill Mixer